Available online at www.sciencedirect.com
SCIENCE DIRECT®
Chaos, Solitons and Fractals 28 (2006) 822–833
CHAOS SOLITONS & FRACTALS
www.elsevier.com/locate/chaos

Determining the flexibility of regular and chaotic attractors

Marko Marhl *, Matjaž Perc

Department of Physics, Faculty of Education, University of Maribor, Koroška cesta 160, SI-2000 Maribor, Slovenia

Accepted 8 August 2005

Abstract

We present an overview of measures that are appropriate for determining the flexibility of regular and chaotic attractors. In particular, we focus on those system properties that constitute its responses to external perturbations. We deploy a systematic approach, first introducing the simplest measure given by the local divergence of the system along the attractor, and then develop more rigorous mathematical tools for estimating the flexibility of the system's dynamics. The presented measures are tested on the regular Brusselator and chaotic Hindmarsh–Rose model of an excitable neuron with equal success, thus indicating the overall effectiveness and wide applicability range of the proposed theory. Since responses of dynamical systems to external signals are crucial in several scientific disciplines, and especially in natural sciences, we discuss several important aspects and biological implications of obtained results.

1. Introduction

There exist several theoretical as well as experimental studies investigating responses of dynamical systems to external perturbations such as noise, periodic inputs or step like pulses, for example. In dependence on the properties of a given dynamical system and the applied external perturbation, responses can vary extremely, ranging from practically no effects to suppressed or enhanced spectral responses of threshold-crossing events [1], regularisation of chaotic states [2–8], chaotification [9–18], or synchronisation of coupled oscillators [19–21], only to mention some of the more prominent examples. In particular in biological systems, responses to external perturbations are of crucial importance since they are vital for flawless functioning of living organisms. For example, the addition of noise amplifies weak external input signals and herewith facilitates signal detection and transduction in the tissue [22–31]. These phenomena are known as stochastic resonance effects. Moreover, effective responses to external perturbations can lead to synchronous calcium waves in tissue [32,33] already at very low coupling strengths between neighbouring cells [20,21]. This is an extremely important phenomenon, since calcium ions are recognised to be one of the most important second messengers, regulating many cellular processes from egg fertilization to cell death [34,35]. Furthermore, there also exist studies evidencing that noise, besides amplifying weak external signals, can also increase the robustness of biological systems [36], thereby assuring reliable and immutable information processing.

* Corresponding author. Tel.: +386 2 2293643; fax: +386 2 2518180.
E-mail address: marko.marhl@uni-mb.si (M. Marhl).

0960-0779/$ - see front matter © 2005 Elsevier Ltd. All rights reserved.
doi:10.1016/j.chaos.2005.08.013

Since responses of dynamical systems to external forcing can be qualitatively and quantitatively very different, the question arises if it is possible to estimate in advance whether a given system, or its particular state, is more or less susceptible to an applied external perturbation. We refer to the property of a dynamical system that determines the effect of the applied external perturbation on the system dynamics as the flexibility. More precisely, if the system is flexible its susceptibility to external perturbations is very high, meaning that even small-amplitude signals will have a large impact on the system dynamics, whereas if the system is not flexible it remains largely unaffected even by strong perturbations. Although flexibility is a very important system property, little light has been shed on the characteristic quantities of a dynamical system that constitute it. The aim of the present paper is to find and mathematically define the particular system properties that determine the flexibility of an attractor, regardless of its complexity.

In our previous works [17,20,30,37,38], we showed that for a N-dimensional dynamical system given with the vector field $\mathbf{F} = (f_1, f_2, \ldots, f_N)$, the time dependent divergence $\nabla \cdot \mathbf{F}$, termed as the local divergence, is a simple but rather effective measure for determining the flexibility of an attractor. Intuitively, the role of the local divergence in determining response abilities of a dynamical system to external perturbations can be well explained, since the local divergence reflects the contractive properties of an attractor in the phase space. Therefore, if an attractor is locally weakly attractive, i.e. has a close to zero local divergence, it seems much easier to alter its shape, thus favouring responses of a system to external perturbations. However, for complex systems this measure is rather loose and must be accompanied with extensive descriptive explanations in order to define the flexibility of an attractor. Furthermore, there exist special cases where the local divergence can give spurious results, i.e. indicating that the system is not flexible, where in fact it is. Moreover, the local divergence gives only information about the flexibility of the system infinitesimally close to the attractor, whereas it does not provide any information about the surrounding phase space. It also does not provide any information about which phase space direction, with respect to the trajectory that constitutes the attractor, is most susceptible to external perturbations.

In this paper, we present more advanced and sophisticated methods for determining the flexibility of dynamical systems that, in several ways, overcome the above-discussed difficulties. We demonstrate our results on two well-known dynamical systems, namely the Brusselator [39] and the Hindmarsh–Rose model of an excitable neuron [40].

The paper is structured as follows. Section 2 is devoted to the accurate mathematical description of the methods used for determining the flexibility of a dynamical system. In Section 3 we provide a short description of the exemplary dynamical systems [39,40], whereas in Section 4 we present the results. In the last section we discuss merits and limitations of our methods. Additionally, possible applications of the methods in engineering and biological sciences are discussed.

2. Methods

2.1. External forcing

The flexibility of a given dynamical system $\mathbf{F} = (f_1, f_2, \ldots, f_N)$ is studied in response to an external forcing that takes the form of an additional flux J that is introduced to a particular system variable x_i. Accordingly, the corresponding differential equation $f_i = \mathrm{d}x_i/\mathrm{d}t$ is replaced by:

$$f_i \Rightarrow f_i + J. \tag{1}$$

In all calculations, we use a simple square-shaped external forcing of the form

$$J(t) = h\begin{cases} 1, & \text{if } (t > t_s) \text{ and } (t < t_s + \tau_d), \\ 0, & \text{else}, \end{cases} \tag{2}$$

where h is the amplitude of the forcing signal, t_s is the starting time of the pulse, and τ_d is the pulse duration.

2.2. Methods for determining the flexibility

Flexibility is a measure for the susceptibility of a dynamical system to external forcing. Flexible systems are susceptible to weak external perturbations and can better adjust their behaviour in accordance with the external signal. In general, the sum of all Lyapunov exponents (λ_i, where $i \in \{1, \ldots, N\}$; N is the dimension of the phase space) can be introduced as an appropriate quantity for determining the flexibility of regular as well as chaotic attractors. Crucial thereby is the fact, that we calculate the Lyapunov exponents locally along the attractor. These locally defined Lyapunov exponents give information about the attractive properties of particular parts of the attractor. The sum of all

Lyapunov exponents at a given time corresponds to the so-called local divergence of the vector field $\mathbf{F} = (f_1, f_2, \ldots, f_N)$, and thus represents the volume contraction in the phase space:

$$\mathrm{Flex}_1 = \nabla \cdot \mathbf{F} = \sum_i \lambda_i. \tag{3}$$

As already advocated [17,20,30,37,38], Flex_1 is a universal but rather rough measure for estimating the flexibility of an attractor. In particular, it is very appropriate for systems with a nearly constant vector field norm along the trajectory (tr), i.e. $\|\mathbf{F}\|_{\mathrm{tr}} \approx \text{const}$. In this case the Lyapunov exponent λ_{tr}, measuring the contraction of the phase space along the trajectory, is close to zero at any time, i.e. in addition to $\langle \lambda_{\mathrm{tr}} \rangle = 0$ for periodic orbits, also $\lambda_{\mathrm{tr}}(t) \approx 0$ at any time t. In such cases:

$$\mathrm{Flex}_1 \approx \mathrm{Flex}_2 = \sum_j \lambda_j, \quad \text{for } j \in \{1, \ldots, N\} \wedge j \neq \mathrm{tr}. \tag{4}$$

For dynamical systems with time scale separation, where $\|\mathbf{F}\|_{\mathrm{tr}} \lesseqgtr \text{const}$. and $\lambda_{\mathrm{tr}}(t) \lesseqgtr 0$, the flexibility of the corresponding attractor is more accurately given by Flex_2 rather than Flex_1. However, since the trajectory of systems with time scale separation, as are for example relaxation oscillators, moves through certain phase space areas very fast, Flex_2 still cannot be considered as the fully appropriate quantity for determining the flexibility of the attractor. The problem lies in the fact that the time τ_{d} in which J acts on the dynamics can be considerably longer than the typical time the system needs to sweep through the phase space. Accordingly, the flexibility of the attractor at time t_{s} can be vastly different from the flexibility at time $t_{\mathrm{s}} + \tau_{\mathrm{d}}$. Thus, to get the most accurate measure for the flexibility also in cases where $\|\mathbf{F}\|_{\mathrm{tr}} \lesseqgtr \text{const}$. and $\lambda_{\mathrm{tr}}(t) \lesseqgtr 0$, we define the flexibility of an attractor Flex_3 as $\mathrm{Flex}_3 = \langle \mathrm{Flex}_2 \rangle$ calculated at a particular time t for the period τ_{d} according to the equation:

$$\mathrm{Flex}_3 = \langle \mathrm{Flex}_2 \rangle = \frac{1}{\tau_{\mathrm{d}}} \int_t^{t+\tau_{\mathrm{d}}} \left(\sum_j \lambda_j \right) \mathrm{d}t, \quad \text{for } j \in \{1, \ldots, N\} \wedge j \neq \mathrm{tr}. \tag{5}$$

If in addition to $\|\mathbf{F}\|_{\mathrm{tr}} \lesseqgtr \text{const}$. and $\lambda_{\mathrm{tr}}(t) \lesseqgtr 0$, some phase space dimensions, denoted by $j = \mathrm{ext}$, are characterized by extreme values of Lyapunov exponents, i.e. λ_{ext} have much higher/lower values than other λ_j, which can be the case in higher dimensional systems, the flexibility has to be evaluated very carefully by taking all λ_{ext} into account separately, whilst calculating the sum of all other λ_j according to:

$$\mathrm{Flex}_4 = \frac{1}{\tau_{\mathrm{d}}} \int_t^{t+\tau_{\mathrm{d}}} \left(\sum_j \lambda_j \right) \mathrm{d}t, \quad \text{for } j \in \{1, \ldots, N\} \wedge j \neq \mathrm{tr} \wedge j \neq \mathrm{ext}. \tag{6}$$

For the separate consideration of λ_{ext} the average values $\langle \lambda_{\mathrm{ext}} \rangle$ have to be calculated, identically as for other λ_j, during time τ_{d}, in which $J \lesseqgtr 0$. Only for these λ_{ext} that satisfy $|\langle \lambda_{\mathrm{ext}} \rangle| \gg |\lambda_j|$, $j \in \{1, \ldots, N\} \wedge j \neq \mathrm{tr} \wedge j \neq \mathrm{ext}$, the effects of $\langle \lambda_{\mathrm{ext}} \rangle$ have to be treated separately, whereas otherwise λ_{ext} can be included into the sum as in Eq. (5).

3. Mathematical models

The above-presented methods for determining the flexibility of regular and chaotic attractors will be applied on two well known dynamical systems; namely the Brusselator [39] and the Hindmarsh–Rose model of an excitable neuron [40], which are described next.

3.1. Brusselator

The Brusselator [39] is a widely used model for describing autocatalytic chemical reactions of the form: $2X + Y \rightarrow 3X$, which describe self-production of substance X (activator) under the control of substance Y (inhibitor). The simplest autocatalytic model scheme can be described with the following equations:

$$\frac{\mathrm{d}x}{\mathrm{d}t} = \frac{1}{\tau_x}(1 - (A+1)x + yx^2), \tag{7}$$

$$\frac{\mathrm{d}y}{\mathrm{d}t} = \frac{1}{\tau_y}(Ax - yx^2), \tag{8}$$

where x and y are the concentrations of the activator and the inhibitor, respectively; τ_x and τ_y determine the time scales of x and y, whereas A is the control parameter. In our calculations, we use the parameter values: $\tau_x = 1$, $\tau_y = 100$ and

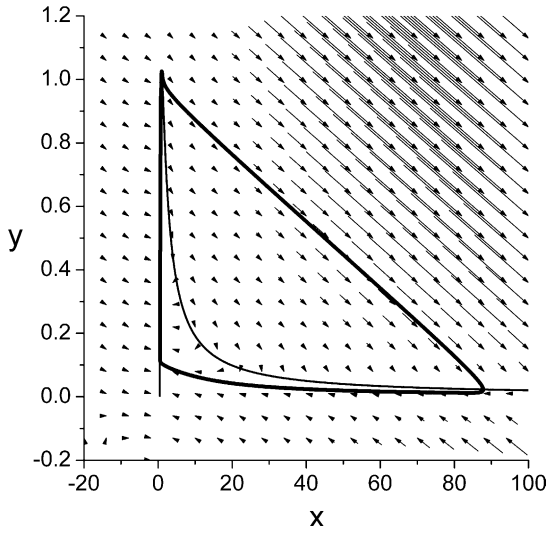

Fig. 1. Phase space analysis of the Brusselator. Arrows represent the vector field of the system, whilst the thin solid line denotes the nullcline of variable x. For parameter values see text.

$A = 1.02$. The corresponding limit cycle attractor together with the vector field and the nullcline of Eq. (7) is presented in Fig. 1. The nullcline of Eq. (7), obtained as the solution $y(x)|_{dx/dt=0}$, has a Λ-like shape and comes very close to the limit cycle at the upper left corner, which strongly indicates that the system is characterised by relaxation oscillations.

3.2. Hindmarsh–Rose model

The Hindmarsh–Rose (HR) model of an excitable neuron [40] is a polynomial model derived from the Hodgin–Huxley (HH) equations [41]. Generally, the polynomial form of the HR model is much more convenient, both for the mathematical analysis as well as numerical simulations, in comparison to the more physiological HH-type models. Fascinatingly, Osipov and Ponizovskaya [42,43] have showed that the traditional HR equations can be simplified even further, finally obtaining the equations:

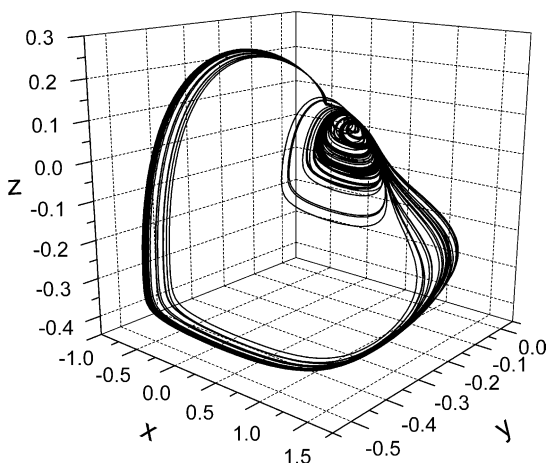

Fig. 2. Three-dimensional chaotic attractor of the Hindmarsh–Rose model. For parameter values see text.

$$\frac{dx}{dt} = \frac{1}{\tau_x}(-\tau_x x + y - ax^3 + bx^2 + z), \tag{9}$$

$$\frac{dy}{dt} = -ax^3 - (d-b)x^2 + z, \tag{10}$$

$$\frac{dz}{dt} = \frac{1}{\tau_z}(-sx - z + c). \tag{11}$$

For a detailed explanation of the derivation and the particular meaning of the variables and parameters we refer the reader to the original articles [42,43]. In our calculations, we use parameter values: $\tau_x = 0.03$, $\tau_z = 0.8$, $a = 0.49$, $b = d = s = 1.0$ and $c = 0.0322$. For the given parameter values, the system exhibits chaotic behaviour, as presented in Fig. 2.

4. Results

4.1. Results for the Brusselator

The Brusselator is a rather simple dynamical system with some obvious properties concerning the response abilities to external perturbations, which were already studied in the past [44,45]. Here, we use the model for demonstrating the effectiveness of our methods defined in Section 2.2, and to show the relationship with the previous related approaches such as the bifurcation analysis [46,47] and the nullcline based insights.

We start by demonstrating the effectiveness of the first measure of the flexibility ($Flex_1$), which states that the local divergence can be used for estimating the flexibility of a dynamical system. Obtained results are shown in Fig. 3. The step-like external forcing (Eq. (2)) is systematically applied during one oscillation period. The dashed line in Fig. 3(a) and (b) represents the boundary between the flexible region in which the system responds to the external forcing with a

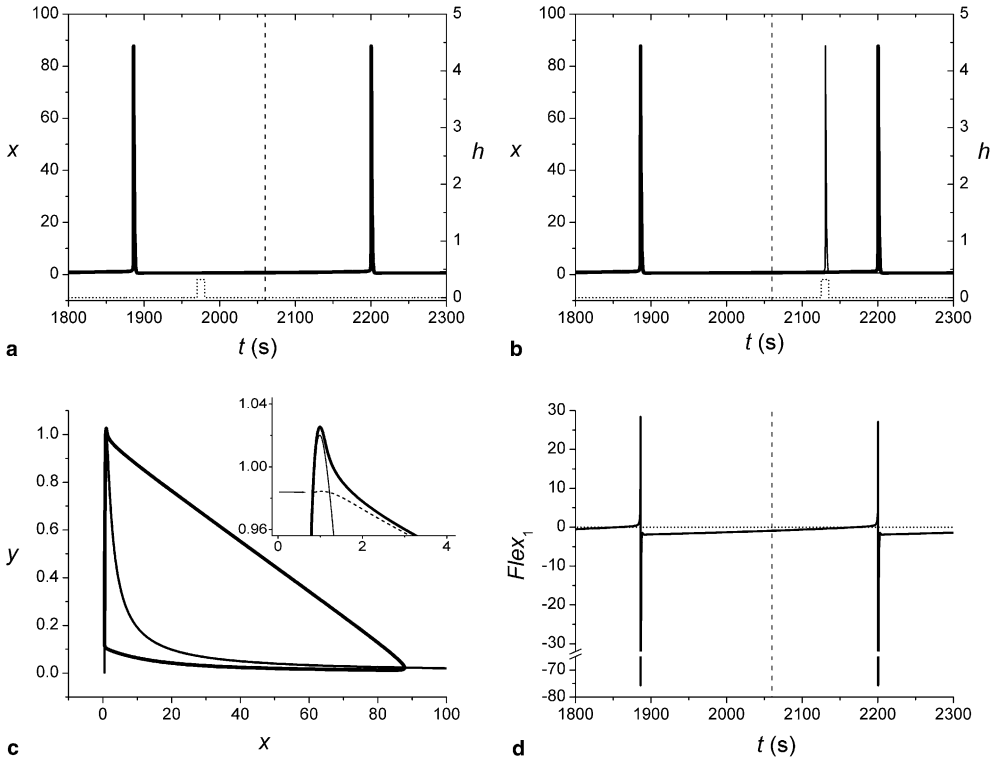

Fig. 3. Application of the flexibility measure $Flex_1$ on the Brusselator. (a) Forcing in the rigid part of the attractor. (b) Forcing in the flexible part of the attractor. (c) Phase space view of Fig. 3(b). (d) Time course of local divergence ($Flex_1$) for one oscillation period. Parameter values for the forcing signal: $\tau_d = 10.0$ and $h = 0.32$.

new spike and the robust region in which there is no considerable response. Fig. 3(c) shows the phase space view of the system's response presented in Fig. 3(b). In particular, the inset of Fig. 3(c) shows the emergence of a new premature spike in the phase space. The arrow denotes the application of the external forcing. To explain the appearance of a new spike in the flexible part of the attractor, we calculate the local divergence (Flex_1) along the whole limit cycle. Results are shown in Fig. 3(d). It can be well observed that the flexible part of the attractor is characterised by close to zero local divergence ($\mathrm{Flex}_1 \approx 0$). Thus, the phase space there is weakly contractive, which facilitates responses even to very weak external signals. In the robust part, which is characterised by more negative values of Flex_1, the contraction of the phase space around the limit cycle is stronger, so that the applied weak external forcing cannot induce a considerable response of the system in the sense of a new spike.

By calculating Flex_1, the flexibility of a dynamical system is estimated by considering the different contraction properties of the phase space along the attractor. This is a simple and very useful measure for the flexibility if $\lambda_{\mathrm{tr}}(t) \approx 0$ or if λ_{tr} is negligible in comparison with the sum of all Lyapunov exponents. In general, the flexibility of a system depends significantly only on the contraction properties of the phase space orthogonal towards the trajectory, whilst phase space contractions along the trajectory, should not be taken into account. Therefore, for estimating the flexibility of dynamical systems, only those Lyapunov exponents that are orthogonal to the tangent of the trajectory λ_j, where $j \in \{1,\ldots,N\} \wedge j \neq \mathrm{tr}$, have to be taken into account. This consideration results in an improved measure for the system's flexibility Flex_2, as given with Eq. (4). Since the Brusselator is only two-dimensional, only the second Lyapunov exponent (λ_2) determines the phase space contraction along the trajectory, and thus $\mathrm{Flex}_2 = \lambda_2$. The results are presented in the phase space as grey-scaled stripes along the trajectory, where the grey intensity represents the strength of the contraction (C_1) orthogonal to the trajectory and is calculated according to the equation:

$$C_1 = -\sum_j \lambda_j \|\Delta \mathbf{r}\|, \tag{12}$$

where $\|\Delta \mathbf{r}\|$ is the square norm of the distance orthogonal to the trajectory. Thereby, we get a topological picture of the phase space where the grey intensity represents the landscape around the trajectory. If the sign of the C_1 is positive, we can imagine a $\vee$-shaped canyon surrounding the trajectory, whereby the depth is determined by the sum of the orthogonal Lyapunov exponents λ_j (in our case only λ_2). The larger the positive value of C_1 is, the more difficult it is to force the trajectory away from its originally determined path. If on the other hand C_1 is negative, it can be imagined that the trajectory moves on a $\wedge$-shaped hill. Thus, even a small perturbation results in a more or less large excursion of the trajectory depending on the value of C_1. Results, together with the applied forcing at several different times, are presented in Fig. 4. Basically, they reflect the results presented in Fig. 3. Nevertheless, Fig. 4 reveals two interesting phenomena that need to be explained further. First, the direction of the forcing signal (the sign of h) is not irrelevant with respect to the forcing effect. From Fig. 4(a) it can be well observed that the forcing signals with $h > 0$ (thick dotted lines) evoke much larger excursion of the trajectory as in the case when $h < 0$ (thin dotted lines). This indicates that in fact the approximation given by C_1 is not completely accurate, and thus the true topology of the phase space around the trajectory is more complicated, i.e. obviously it is not symmetric, but asymmetric. Second, the calculations of C_1 also predict that the largest excursions of the trajectory should be obtained when the system is forced on the descending diagonal part of the trajectory (Fig. 4(b)) where the phase space is divergent (note that C_1 is negative in this part of the limit cycle). However, when the same forcing signal as in Fig. 4(a) is applied to this part of the limit cycle, virtually no excursion of the trajectory away from its originally determined path can be observed. Due to these anomalies there still exists the need for further improvements concerning the above-presented measures for the flexibility of the dynamical system.

To improve the estimation of the flexibility of a dynamical system, we have to take into account also the speed of the trajectory along the attractor. If namely the speed of the trajectory in a given phase space point is very high, Flex_2 is not an appropriate measure for the flexibility of the system in that particular point because the system's dynamics might undergo extensive changes during the forcing time τ_{d}. Thus, to get an appropriate measure for the flexibility also in cases where $\|\mathbf{F}\|_{\mathrm{tr}} \lesseqgtr \text{const.}$ and $\lambda_{\mathrm{tr}}(t) \lesseqgtr 0$, we use the measure $\mathrm{Flex}_3 = \langle \mathrm{Flex}_2 \rangle$, as given with Eq. (5). The effectiveness of Flex_3 in comparison to Flex_2 is presented in Fig. 5. It can be well observed that in Fig. 5(b) the positive divergent parts of the limit cycle (see Fig. 5(a)) disappear, which indicates that the trajectory moves through the corresponding parts of the phase space very fast, whereby the divergent parts average out. Since the duration of the divergent part is much shorter than the duration of the attractive part, the whole section of the trajectory is still very robust to external perturbations, and hence no excursions can be obtained in this part of the limit cycle. This result gives us a good explanation why the applied external forcing in the descending diagonal part of the limit cycle (see Fig. 4(b)) does not evoke any excursions of the trajectory away from its originally determined path, although $\mathrm{Flex}_2 > 0$.

Another question arising in Fig. 4(a) was, why the forcing signals with $h > 0$ (marked with thick dotted lines) evoke much larger excursion of the trajectory as in the case when $h < 0$ (marked with thin dotted lines). This behaviour

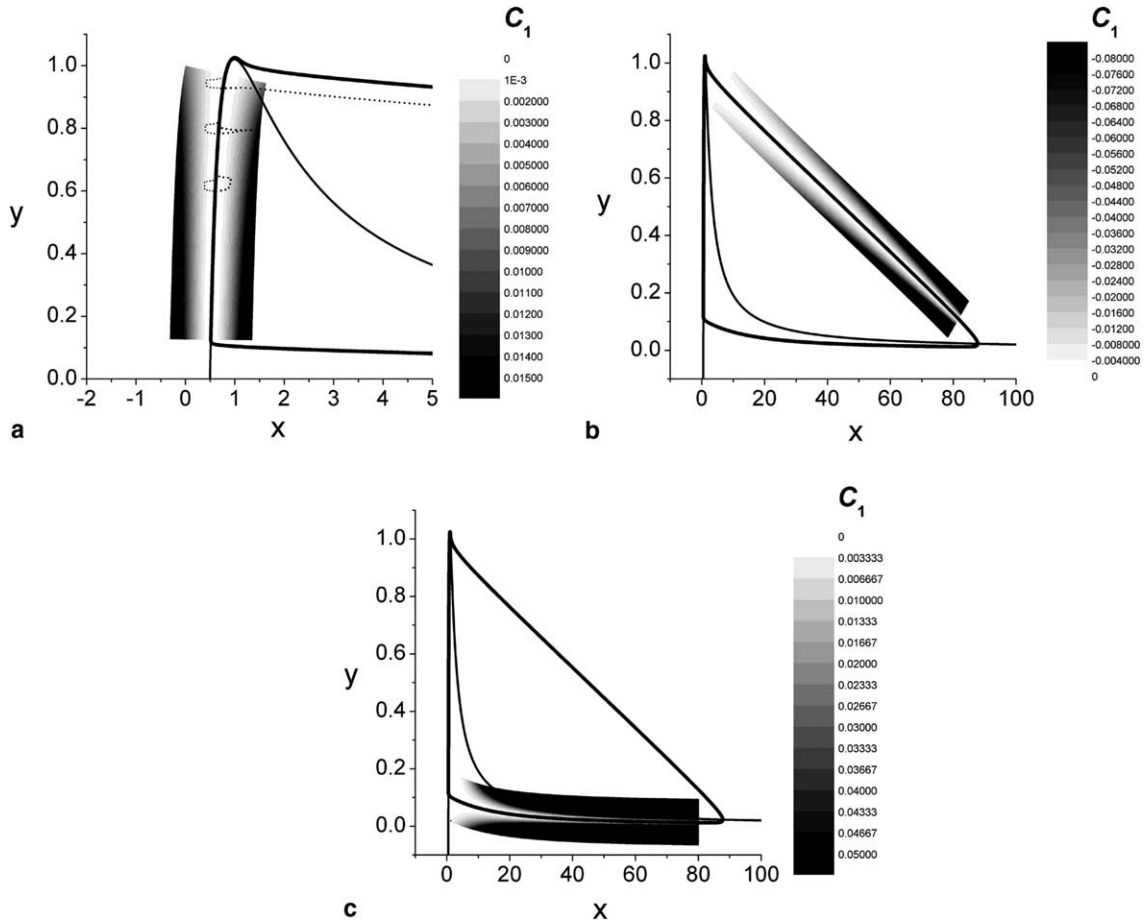

Fig. 4. Application of the flexibility measure Flex_2 on the Brusselator for various parts of the attractor. Thick dotted lines in (a) show the impact of forcing for $\tau_d = 10.0$ and $h = 0.32$, whilst thin dotted lines represent forcing effects for $\tau_d = 10.0$ and $h = -0.32$.

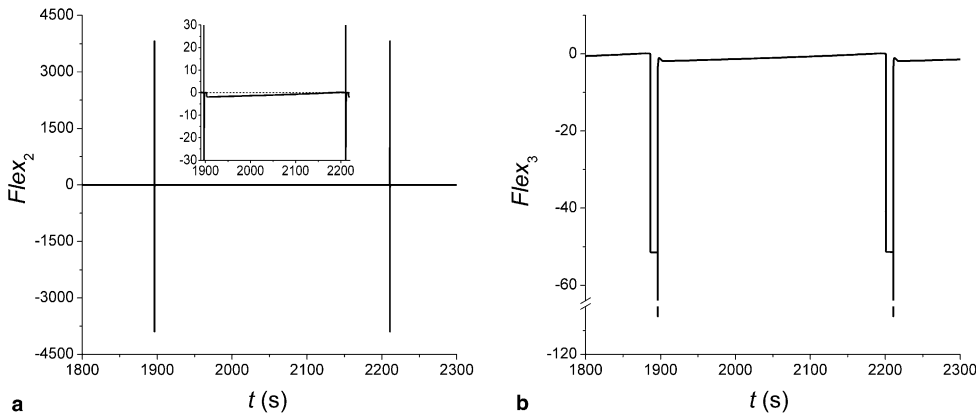

Fig. 5. Comparison of the flexibility measures Flex_2 (a) and Flex_3 (b) for one oscillation period of the Brusselator.

indicates that the topology of the phase space around the trajectory is asymmetric. However, the asymmetry cannot be obtained by the mathematical measures defined by Eqs. (3)–(6) because the Lyapunov exponents represent the contraction of the phase space only infinitesimally close to the trajectory. Therefore, results presented in Fig. 4 are only valid

for $\|\Delta\mathbf{r}\| < \varepsilon$, where $\varepsilon \to 0$. In other words, the true topology of the surrounding phase space at the same distance away from the trajectory as shown in Fig. 4 is in fact very different. In order to see the true topological picture of the phase space, we must calculate the norm of the vector field component orthogonal to the trajectory in every point of the phase space according to the equation:

$$C_2 = \mathbf{F} \cdot \Delta\hat{\mathbf{r}}. \tag{13}$$

The results are presented in Fig. 6, where similarly as in Fig. 4 the grey-scale with assigned positive values represent up-hills, i.e. obstacles that hinder effects of the applied forcing signal. In the left part of Fig. 6, it can be well observed that the phase space to the left of the trajectory is steeper than to the right and thus excursions of the trajectory for $h > 0$ (thick dotted lines) are more expressed than for $h < 0$ (thin dotted lines).

Despite the fact that the above analysis provides a very deep insight into the dynamics of the mathematical model, presenting such results for more than two-dimensional dynamical systems is very difficult and requires special techniques. The biggest obstacle thereby represents the graphical presentation of obtained results. Note that for more than two-dimensional systems phase space portraits are often entangled, as for example shown in Fig. 2. Nevertheless, we believe that the results presented for such relatively simple dynamical systems as is the Brusselator are very enlightening and persuasive, and thus the basic concept is worth developing further.

4.2. Results for the Hindmarsh–Rose model

As by the Brusselator, we first use the simplest approach in order to determine the flexibility of the system. In particular, we calculate the local divergence along the trajectory of the chaotic attractor Flex_1, as given by Eq. (3). The time course of x and the corresponding local divergence are presented in Fig. 7(a) and (b). Because, for the chosen parameter values, the Hindmarsh–Rose model has a more complex dynamics than the Brusselator, these results are not as transparent in terms of determining the flexibility of the system as in the previous case. The non-flexible areas of the attractor characterized by well-expressed negative dells of local divergence are clearly visible, whereas the flexible parts are not so obvious.

To shed more light on the flexibility of the chaotic attractor, we take into account only the Lyapunov exponents that are orthogonal to the tangent of the trajectory, which are λ_2 and λ_3, and consider the speed of the trajectory along the attractor by averaging the sum of the Lyapunov exponents over the forcing time $\tau_d = 1.0$ (see Fig. 8). Thus, the flexibility measure Flex_3 as given by Eq. (5) is applied. The results are presented in Fig. 7(c), where positive (point A) and close to zero (point B) parts of the time course of Flex_3 represent the most flexible parts of the attractor, whereas the negative parts (points C and D) represent more rigid, i.e. non-flexible areas of the phase space, which are difficult to affect directly by the external forcing.

To demonstrate the effectiveness of the flexibility measure Flex_3, we apply the external forcing in points A, B, C and D of the time course as indicated by the arrows in Fig. 7(c). At all four points the duration of the pulse is kept constant ($\tau_d = 1.0$), whereas the amplitude of the external signal increases from point A to D. The increase of the

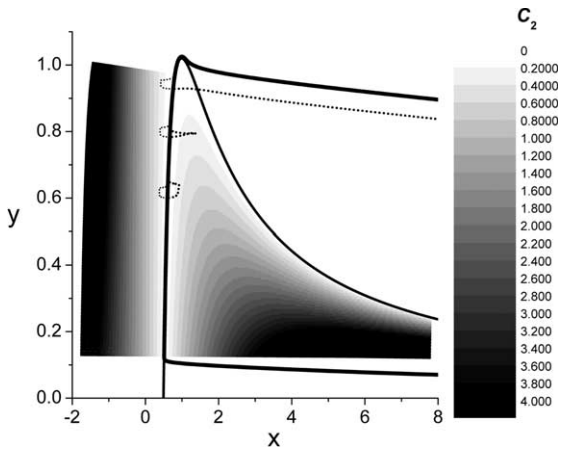

Fig. 6. Orthogonal vector field component analysis of the Brusselator. The thin solid line denotes the nullcline of variable x, whereas thick and thin dotted lines show impacts of various external perturbations for the same parameter values as in Fig. 4(a).

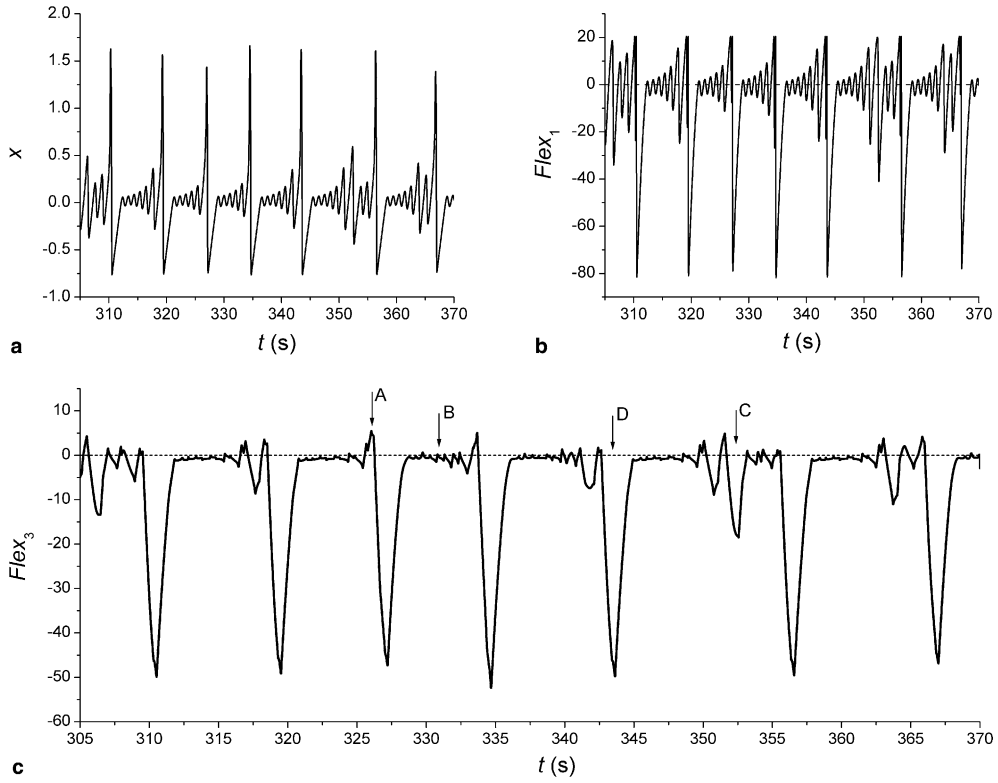

Fig. 7. Application of the flexibility measures $Flex_1$ and $Flex_3$ on the Hindmarsh–Rose model. (a) Time course of variable x. (b) Time course of local divergence ($Flex_1$). (c) Time course of $Flex_3$, whereby arrows indicate times at which the external forcing is applied in Fig. 8.

forcing amplitude h from the point A towards D has been introduced in order to increase the persuasiveness of presented results and to add more credibility to the applied flexibility measure. $Flex_3$ namely predicts that at point A the system is most flexible, whilst it becomes more and more rigid towards D. Results presented in Fig. 8 show that this is indeed true even in the case of increasing amplitudes of the external forcing.

Before evaluating the results presented in Fig. 8 in more detail, it is important to keep in mind the key property of chaos, which is the extreme sensitivity to changes in initial conditions. Thus, every applied external signal, regardless of its amplitude and duration will, as time progresses, induce discrepancies between the perturbed (thick solid line in Fig. 8) and unperturbed trajectory (thin solid line in Fig. 8). Thus, in order to evaluate solely the effects of the external forcing and not the intrinsic dynamics of the system, one has to consider the difference that emerges between the perturbed and unperturbed trajectory immediately after the applied perturbation, since the latter discrepancy is the direct consequence of the external signal. The results in Fig. 8 fully confirm the predictions regarding the system's flexibility that where inferred from Fig. 7(c). It can be well observed that at point A already a small-amplitude forcing immediately evokes a new spike in the time course of x, whereas at point C, for example, even a more than three times stronger external signal cannot induce the same perturbation. Furthermore, at point D the immediate impact of an even stronger external perturbation is extremely minute, which confirms the prediction that the system is very rigid at that point. Note that the induced discrepancy becomes eligible only after one whole oscillation cycle, which is, however, solely the consequence of the system's chaotic dynamics. In summary, results presented in Fig. 8 clearly underline the successfulness of the applied flexibility measure $Flex_3$ also for chaotic systems, thus confirming its overall effectiveness and wide applicability range.

5. Discussion

We present four different measures for determining the flexibility of regular and chaotic attractors. The most straightforward measure, given by the local divergence of the system along the attractor ($Flex_1$), provides useful

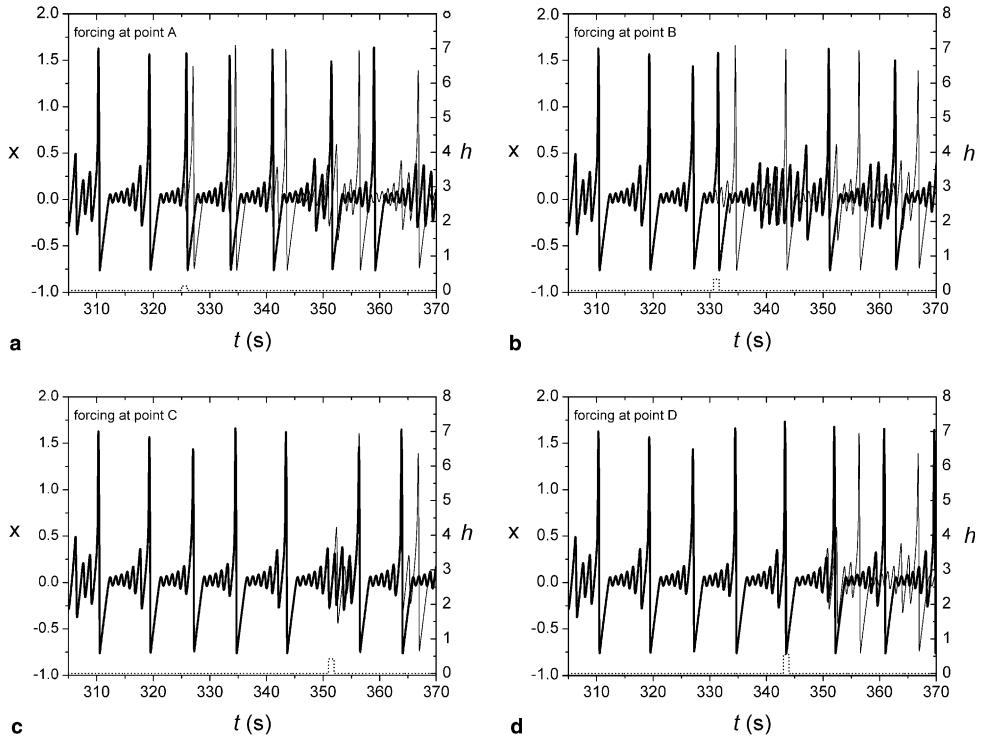

Fig. 8. Effects of external forcing on the Hindmarsh–Rose model at various times denoted by arrows in Fig. 7(c): (a) $\tau_d = 1.0$ and $h = 0.13$, (b) $\tau_d = 1.0$ and $h = 0.33$, (c) $\tau_d = 1.0$ and $h = 0.42$, (d) $\tau_d = 1.0$ and $h = 0.55$.

insights, especially for simple oscillators, whereas for complex systems it must be accompanied by additional descriptive explanations or replaced by more powerful mathematical measures. As the first improvement, we propose to eliminate from the sum of all Lyapunov exponents, giving the local divergence of the system, those that measure the contraction of the phase space along the trajectory. Thereby, we obtain the flexibility measure Flex_2. Similarly as Flex_1, however, the latter also suffers from the fact that during the forcing time, the system's dynamics might change substantially, which is especially true for system with time-scale separation. Thus, in such cases the local measures Flex_1 and Flex_2 are not appropriate since they do not take into account the speed of the trajectory along the attractor. To overcome this deficiency, as the second improvement, we propose to integrate Flex_2 over the duration of the forcing time, thus yielding $\mathrm{Flex}_3 = \langle \mathrm{Flex}_2 \rangle$, which can be considered as the most appropriate and widely applicable measure for determining the flexibility of regular as well as chaotic attractors, while still being fairly easy to implement. Nevertheless, Flex_3 also has some debility, and can be improved further. In particular, since it relies on the Lyapunov exponents, it provides information about the contraction/divergence of the phase space only infinitesimally close to the trajectory, and gives no insights on the surrounding phase space. This information, on the other hand, can be obtained by calculating the vector field component orthogonal to the trajectory, whereby the true phase space topology can be made visible. However, the task of presenting such results for more than two-dimensional systems is rather difficult, and so the development of appropriate graphical tools is left for future studies.

Furthermore, we also outlined an appropriate approach for higher dimensional systems (Flex_4), where it can occur that only one or few Lyapunov exponents have very negative values, whilst all others are close to zero. In such cases, the values of all above-discussed measures (Flex_1, Flex_2, and Flex_3) would still be very negative, thus indicating a very rigid system, which cannot be easily altered by an external forcing. Nevertheless, this interpretation would be false, since in this case the system still has many degrees of freedom that are very susceptible to external perturbations (directions characterized by close to zero Lyapunov exponents), with only one or few rigid phase space directions. Thus, for higher dimensional systems, it is advisable to calculate Flex_4, which means that in the sum of Lyapunov exponents all non-extreme Lyapunov exponents are included, whereas the remaining degrees of freedom are evaluated separately for the flexibility.

The flexibility of a dynamical system is a key property since it constitutes responses to external perturbations, which are omnipresent and affect the functioning of artificial as well as biological systems. In making projects for tall building, for example, scientists have to be able to foretell impacts of strong winds, earthquakes, and other natural forces on the building, since thereon often rely lives of many people. Even more importantly, the nowadays ever-present wireless communication technologies have made electromagnetic radiation a permanent companion of our every day lives. Obviously, it is of outstanding importance to understand how such external influences might affect the functioning of the human brain, as well as other organs and cells in living organisms. Interestingly, controlled external perturbations may be used to improve the performance of biological systems, either by restoring normal, i.e. healthy, system functioning or enhancing their overall effectiveness. It has been shown experimentally that external electromagnetic fields can facilitate cartilage growth and bone healing [48–52]. On the cellular level, it has been found that the electrically stimulated Ca^{2+} influx into the human oocytes can resume apparently normal fertilisation and early embryonic development in the oocytes that fail to fertilize after intracytoplasmic sperm injection [53]. Other well-known examples of positive influences on functioning of whole organs are also reanimation of the human heart with electroshocks [54], or treatments of psychic diseases with electric stimuli applied to the brain [55], for example. All these phenomena have not yet been fully explained by the scientific community. While the reanimation of the human heart with strong electroshocks may seem self-explanatory and has been used successfully for many decades, other phenomena seem to have more intriguing background and are subject of fearsome debate [56]. Although answers to the above questions are often sought and obtained experimentally, mathematical modelling might be the tool-of-choice for the future, providing insights that are currently not attainable experimentally, or outlining innovative directions for future experimental work, whereby the determination of flexibility of resulting mathematical models will be of crucial importance.

References

[1] Gammaitoni L, Hänggi P, Jung P, Marchesoni F. Stochastic resonance. Rev Mod Phys 1998;70:223–87.
[2] Lima R, Pettini M. Suppression of chaos by resonant parametric perturbations. Phys Rev A 1990;41:726–33.
[3] Braiman Y, Goldhirsch J. Taming chaotic dynamics with weak periodic perturbations. Phys Rev Lett 1991;66:2545–8.
[4] Kapitaniak T. Continuous control and synchronization in chaotic systems. Chaos, Solitons & Fractals 1995;6:237–44.
[5] Brindley J, Kapitaniak T, Kocarev L. Controlling chaos by chaos in geophysical systems. Geophys Res Lett 1995;22:1257–60.
[6] Kapitaniak T. Chaos for engineers: theory, applications and control. Berlin: Springer; 1998.
[7] Chen G, Dong X. From chaos to order: methodologies, perspectives and applications. Singapore: World Scientific; 1998.
[8] Boccaletti S, Grebogi C, Lai Y-C, Mancini H, Maza D. The control of chaos: theory and applications. Phys Rep 2000;329:103–97.
[9] Yang W, Ding M, Mandell AJ, Ott E. Preserving chaos: control strategies to preserve complex dynamics with potential relevance to biological disorders. Phys Rev E 1995;51:102–10.
[10] Yang L, Liu Z, Chen G. Chaotifying a continuous-time system via impulsive input. Int J Bifurcat Chaos 2002;12:1121–8.
[11] Codreanu S. Desynchronization and chaotification of nonlinear dynamical systems. Chaos, Solitons & Fractals 2002;13:839–43.
[12] Chen G, Yang L. Chaotifying a continuous-time system near a stable limit cycle. Chaos, Solitons & Fractals 2003;15:245–53.
[13] Li C, Chen G. On the Marotto–Li–Chen theorem and its application to chaotification of multi-dimensional discrete dynamical systems. Chaos, Solitons & Fractals 2003;18:807–17.
[14] Li C. On super-chaotifying discrete dynamical systems. Chaos, Solitons & Fractals 2004;21:855–61.
[15] Chen H-K, Lee C-I. Anti-control of chaos in rigid body motion. Chaos, Solitons & Fractals 2004;21:957–65.
[16] Starkov K, Chen G. Chaotification of polynomial continuous-time systems and rational normal forms. Chaos, Solitons & Fractals 2004;22:849–56.
[17] Perc M, Marhl M. Detecting and controlling unstable periodic orbits that are not part of a chaotic attractor. Phys Rev E 2004;70:016204.
[18] Perc M, Marhl M. Chaos in temporarily destabilized regular systems with the slow passage effect. Chaos, Solitons & Fractals 2006;27:395–403.
[19] Izhikevich EM. Synchronization of elliptic bursters. SIAM Rev 2001;43:315–44.
[20] Perc M, Marhl M. Synchronization of regular and chaotic oscillations: the role of local divergence and the slow passage effect. A case study on calcium oscillations. Int J Bifurcat Chaos 2004;14:2735–51.
[21] Perc M, Marhl M. Local dissipation and coupling properties of cellular oscillators. A case study on calcium oscillations. Bioelectrochemistry 2004;62:1–10.
[22] Douglass JK, Wilkens LA, Pantazelou E, Moss F. Noise enhancement of information transfer in crayfish mechanoreceptors by stochastic resonance. Nature 1993;365:337–40.
[23] Braun HA, Wissing H, Schäfer K, Hirsch MC. Oscillation and noise determine signal transduction in shark multimodal sensory cells. Nature 1994;367:270–3.
[24] Morse RP, Evans EF. Enhancement of vowel coding for cochlear implants by addition of noise. Nat Med 1996;2:928–32.
[25] Kanamaru T, Okabe Y. Stochastic resonance in a pulse neural network with a propagational time delay. BioSystems 2000;58:101–7.

[26] Zhang J, Qi F, Xin H. Effects of noise on the off rate of Ca^{2+} binding proteins in a coupled biochemical cell system. Biophys Chem 2001;94:201–7.
[27] Manjarrez E, Diez-Martinez O, Mendez I, Flores A. Stochastic resonance in human electroencephalographic activity elicited by mechanical tactile stimuli. Neurosci Lett 2002;324:213–6.
[28] Hänggi P. Stochastic resonance in biology. How noise can enhance detection of weak signals and help improve biological information processing. Chem Phys Chem 2002;12:285–90.
[29] Reinker S, Puil E, Miura RM. Resonances and noise in a stochastic Hindmarsh–Rose model of thalamic neurons. Bull Math Biol 2003;65:641–63.
[30] Perc M, Marhl M. Frequency dependent stochastic resonance in a model for intracellular Ca^{2+} oscillations can be explained by local divergence. Physica A 2004;332:123–40.
[31] Perc M, Marhl M. Amplification of information transfer in excitable systems that reside in a steady state near a bifurcation point to complex oscillatory behavior. Phys Rev E 2005;71:026229.
[32] Berridge MJ, Dupont G. Spatial and temporal signalling by calcium. Curr Opin Cell Biol 1994;6:267–74.
[33] Snita D, Hasal P, Merkim JH. Electric field induced propagating structures in a model of spatio-temporal signalling. Physica D 2000;141:155–69.
[34] Berridge MJ, Bootman MD, Lipp P. Calcium—A life and death signal. Nature 1998;395:645–8.
[35] Schuster S, Marhl M, Höfer T. Modelling of simple and complex calcium oscillations. From single-cell responses to intercellular signalling. Eur J Biochem 2002;269:1333–55.
[36] Perc M, Marhl M. Noise enhances robustness of intracellular Ca^{2+} oscillations. Phys Lett A 2003;316:304–10.
[37] Perc M, Marhl M. Sensitivity and flexibility of regular and chaotic calcium oscillations. Biophys Chem 2003;104:509–22.
[38] Marhl M, Schuster S. Under what conditions signal transduction pathways are highly flexible in response to external forcing? A case study on calcium oscillations. J Theor Biol 2003;224:491–500.
[39] Nicolis G, Prigogine I. Self-organization in nonequilibrium systems. New York: Wiley; 1977.
[40] Hindmarsh JL, Rose RM. A model of neuronal bursting using three coupled first order differential equations. Proc R Soc Lond B 1984;221:87–102.
[41] Hodgin AL, Huxley AF. The dual effect of membrane potential on sodium conductance in the giant axon of Loligo. J Physiol 1952;116:497–506.
[42] Osipov VV, Ponizovskaya EV. Multivalued stochastic resonance in a model of an excitable neuron. Phys Lett A 2000;271:191–7.
[43] Osipov VV, Ponizovskaya EV. The nature of bursting noises, stochastic resonance and deterministic chaos in excitable neurons. Phys Lett A 1998;238:369–74.
[44] Kuramoto Y. Chemical oscillations, waves, and turbulence. Berlin: Springer-Verlag; 1984.
[45] Osipov VV, Ponizovskaya EV. Stochastic resonance in the Brusselator model. Phys Rev E 2000;61:4603–5.
[46] Izhikevich EM. Neural excitability, spiking, and bursting. Int J Bifurcat Chaos 2000;10:1171–266.
[47] Perc M, Marhl M. Different types of bursting calcium oscillations in non-excitable cells. Chaos, Solitons & Fractals 2003;18:759–73.
[48] Torricelli P, Fini M, Giavaresi G, Cane V, Giardino R. In vitro evaluation of the effects of electromagnetic fields used for bone healing. Electro Magnetobiol 1998;17:335–42.
[49] Ciombor DM, Lester G, Aaron RK, Neame P, Caterson B. Low frequency EMF regulates chondrocyte differentiation and expression of matrix proteins. J Orthopaed Res 2002;20:40–50.
[50] Aaron RK, Wang S, Ciombor DM. Upregulation of basal TGF beta(1) levels by EMF coincident with chondrogenesis-implications for skeletal repair and tissue engineering. J Orthopaed Res 2002;20:233–40.
[51] De Mattei M, Pasello M, Pellati A, Stabellini G, Massari L, Gemmati D, et al. Effects of electromagnetic fields on proteoglycan metabolism of bovine articular cartilage explants. Connect Tissue Res 2003;44:154–9.
[52] De Mattei M, Pellati A, Pasello M, Ongaro A, Setti S, Massari L, et al. Effects of physical stimulation with electromagnetic field and insulin growth factor-I treatment on proteoglycan synthesis of bovine articular cartilage. Osteoarthr Cartilage 2004;12:793–800.
[53] Zhang J, Wang CW, Blaszcyzk A, Grifo JA, Ozil J, Haberman E, et al. Electrical activation and in vitro development of human oocytes that fail to fertilize after intracytoplasmic sperm injection. Fertility Sterility 1999;72:509–12.
[54] Temes G, Lantos J, Torok B. Possibility of brain recovery after electrically induced cardiac arrest and reanimation in dogs. Acta Physiol Hung 1987;70:93–103.
[55] Beyer JL, Weiner RD, Glenn MD. Electroconvulsive therapy: a programmed text. Washington: American Psychiatric Press; 1998.
[56] Electroconvulsive therapy. Available from: http://www.psycom.net/depression.central.ect.html.